Quantum Electronics **27** (2) 146 – 149 (1997)

PACS numbers: 42.81.Qb; 42.65.Hw; 42.40.Eq

Photoinduced in-fibre refractive-index gratings for core – cladding mode coupling

S A Vasil'ev¶, E M Dianov, A S Kurkov, O I Medvedkov, V N Protopopov

Abstract. Experimental and theoretical investigations are reported of the spectral characteristics of photoinduced in-fibre refractive-index gratings for coupling the fibre core and cladding modes. A theoretical model is developed for predicting the transmission spectra of such gratings and the structure of the coupled cladding modes is considered.

1. Introduction

Formation of distributed refractive-index (RI) structures in fibre cores has been attracting rapidly growing interest. Such structures are usually formed in germanosilicate fibres by sideways exposure to sufficiently powerful UV radiation of wavelength within the absorption band of germanium oxygen-deficient centres, which has a maximum at $\lambda \approx 242$ nm [1], or to ArF excimer laser radiation with $\lambda = 193$ nm [2]. The resultant in-fibre RI gratings have spectral characteristics which can be used effectively in many practical devices, such as sensors, fibre-laser mirrors, filters, etc. [3].

In contrast to the traditional Bragg gratings, which couple the fundamental guided mode of a fibre to a counterpropagating mode, and whose period is usually a fraction of a micron [3], the recently proposed photoinduced RI gratings have a large period $\Lambda = 100 - 500$ μm [4] and they couple the core modes to the cladding modes propagating in the same direction. As a rule, the cladding modes are guided by the air – silica glass interface laid bare by removing a protective coating from the region to be irradiated. The energy transferred to a cladding mode is then absorbed in the protective coating elsewhere in the fibre, which gives rise to an absorp-tion band in the transmission spectrum of a fibre containing such a grating. Gratings of this kind have already been used in fibre-optic devices [5, 6]. However, the properties of long-period gratings have not yet been investigated sufficiently thoroughly and there is as yet no even approximately comprehensive mathematical description of the gratings.

We shall report the main calculated relationships describing the spectral characteristics of long-period gratings and we shall compare these relationships with experimental results.

¶ This author's name is sometimes spelt Vasiliev in the Western literature.

S A Vasil'ev, E M Dianov, A S Kurkov, O I Medvedkov, V N Protopopov
Scientific Centre for Fibre Optics at the Institute of General Physics, Russian Academy of Sciences, ul. Vavilova 38, 117942 Moscow
Tel. (095) 132 83 06; fax (095) 135 81 39
E-mail: sav@fo.gpi.ac.ru

Received 8 August 1996
Kvantovaya Elektronika **24** (2) 151 – 154 (1997)
Translated by A Tybulewicz

2. Theory

The condition for resonant coupling of a core mode to one of the guided cladding modes is

$$(n_{\text{eff}}^{\text{c}} - n_{\text{eff}}^{\text{cl}})\Lambda = \lambda_{\text{r}} \,, \tag{1}$$

where $n_{\text{eff}}^{\text{c}}$ and $n_{\text{eff}}^{\text{cl}}$ are the effective RIs of the core and cladding modes, respectively; Λ is the grating period; λ_{r} is the resonance wavelength. The effective RIs of the modes in a circular dielectric fibre can be found by solving a two-dimensional wave equation for the field components $E_z(r, \varphi)$ and $H_z(r, \varphi)$ [7], described in a cylindrical coordinate system (z, r, φ):

$$(\nabla^2 + k^2)\begin{Bmatrix} E_z \\ H_z \end{Bmatrix} = 0 \,, \tag{2}$$

where ∇^2 is the Laplace operator; $k^2 = (2\pi/\lambda)^2[n(r)^2 - n_{\text{eff}}^2]$; $n(r)$ is the radial distribution of the RI in the fibre. The method for solving Eqn (2) in the case of a fibre waveguide with a step RI profile is given in Ref. [7]. We shall consider a three-layer structure characterised by

$$n(r) = \begin{cases} n_1 \,, & r < a \,, \\ n_2 \,, & a < r < b \,, \\ n_3 \,, & r > b \,, \end{cases} \tag{3}$$

where a and b are the radii of the fibre core and cladding, respectively; n_1, n_2, and n_3 are the RIs of the core, cladding, and ambient medium, respectively. Without loss of generality, we shall plot the calculated dependences by assuming the parameters of a single-mode fibre waveguide used in our experimental investigation: $\Delta n = n_1 - n_2 = 0.015$; $n_3 = 1$; $2a = 3.4$ μm; $2b = 125$ μm; the cutoff wavelength of the first higher core mode $\lambda_{\text{c}} = 0.93$ μm.

Eqns (2) and (3) make it possible to find the complete set of guided modes HE_{lm} and EH_{lm} (l and m are the azimuthal and radial orders of a mode), among which the only guided core mode with a wavelength $\lambda > \lambda_{\text{c}}$ is HE_{11}. A large number $(\sim 10^4)$ of guided modes may then propagate in the cladding, but only a small portion of these modes has a sufficiently large integral I representing the overlap with a core mode in the region where modulation of the RI is induced (for photoinduced gratings, this region is the germanosilicate core of the fibre):

$$I = \frac{\displaystyle\int_0^a \int_0^{2\pi} E_{\text{c}} E_{\text{cl}}^* r \, \text{d}r \, \text{d}\varphi}{\left(\displaystyle\int_0^\infty \int_0^{2\pi} E_{\text{c}} E_{\text{c}}^* r \, \text{d}r \, \text{d}\varphi\right)^{1/2} \left(\displaystyle\int_0^\infty \int_0^{2\pi} E_{\text{cl}} E_{\text{cl}}^* r \, \text{d}r \, \text{d}\varphi\right)^{1/2}} \,, \tag{4}$$

where E_{c} and E_{cl} are the amplitudes of the electric field of the core and cladding modes, respectively.

The overlap integral I determines the efficiency of intermode conversion and it is large only for the HE_{1m} cladding modes, since only they have a sufficiently high component of the electric field in the fibre core. Therefore, we shall limit our analysis to just these modes. Fig. 1 shows the energy-normalised radial distributions of the electric field for some HE_{1m} modes, obtained by numerical solution of Eqns (2) and (3). These modes are linearly polarised, their intensity distributions have the axial symmetry, and the number of zeroes in the radial direction is $m - 1$.

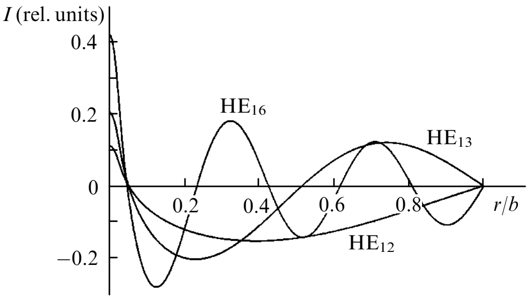

Figure 1. Radial distributions of the amplitudes of the electric fields of the cladding modes HE_{12}, HE_{13}, and HE_{16}.

Fig. 2a gives the dependences of the longitudinal phase parameter $B = (n_{\text{eff}}^2 - n_3^2)/(n_1^2 - n_3^2)$ on the wavelength of the HE_{1m} modes; this figure includes the straight line

$$B = \left[\left(n_{\text{eff}}^{\text{c}} - \frac{\lambda}{\Lambda}\right)^2 - n_3^2\right]\left(n_1^2 - n_3^2\right)^{-1}$$

for $\Lambda = 320$ μm (chain line), representing the geometric locus of points described by condition (1). Intersections of this line with the dependences $B(\lambda)$ for the $HE_{1m}(m > 1)$ modes represent a graphical solution of Eqn (1) and therefore determine the wavelengths λ_{r} of the resonant interaction between the core and cladding modes. This is illustrated in Fig. 2b by the relevant experimental transmission spectrum of a long-period grating.

Eqns (1) – (3) make it possible to find the wavelength of the resonant interaction of these modes, whereas the strength of the interaction and the wavelength dependence of this strength should be found with the aid of coupled-mode equations [8]. The solution of these equations in the approximation of two interacting modes travelling in the same direction (usually, only two modes are sufficiently phase-matched to ensure a significant exchange of energy between them) and in the approximation of smallness of the induced RI gives, for the initial conditions $R(0) = 1$ and $S(0) = 0$, the following energy exchange law:

$$R(z) = \cos^2\left[z(\eta^2 + \delta^2)^{1/2}\right] + \frac{\delta^2}{\eta^2 + \delta^2}\sin^2\left[z(\eta^2 + \delta^2)^{1/2}\right],$$
$$S(z) = \frac{\eta^2}{\eta^2 + \delta^2}\sin^2\left[z(\eta^2 + \delta^2)^{1/2}\right], \quad (5)$$

where $R(z)$ and $S(z)$ are the normalised energies of the core and cladding modes, respectively, considered as a function of the coordinate z along the fibre axis (the grating begins at $z = 0$);

$$\delta = \frac{2\pi\left(n_{\text{eff}}^{\text{c}} - n_{\text{eff}}^{\text{cl}}\right)\text{d}\lambda}{\lambda_{\text{r}}^2} = \frac{2\pi}{\Lambda}\frac{\text{d}\lambda}{\lambda_{\text{r}}}$$

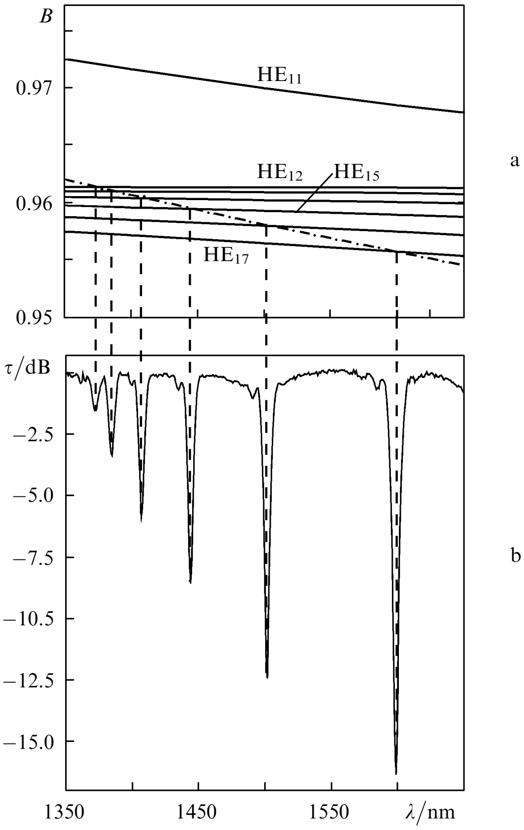

Figure 2. Dependence of the parameter B on the wavelength for the HE_{1m} ($m = 1-7$) modes (a) and the spectrum of the transmission coefficient τ of a photoinduced long-period refractive-index grating (b).

is the normalised frequency describing the deviation from the exact phase matching satisfying condition (1); η is the coupling constant defined as

$$\eta = C\pi\Delta n I \lambda_{\text{r}}^{-1}\,; \quad (6)$$

Δn is the amplitude of modulation of the RI of the core, related to the total change in the RI induced by UV radiation via the expression $\Delta n = \Delta n_{\text{ind}}/2$; C is a constant equal to the first coefficient in the expansion of the profile of a grating line as a Fourier series. If the RI modulation is sinusoidal, this constant is $C = 1$, usually implied in the Bragg grating case [1], when interference of two coherent UV beams is used. The grating line profile of long-period gratings, for example those formed through an amplitude mask, is more likely to be rectangular. We then have $C = 4\sin(\pi d/\Lambda)/\pi$, where d is the size of the illuminated part of the fibre within one grating period.

It therefore follows that we can use Eqns (1) – (6) to find the complete transmission spectrum of a photoinduced RI grating intended for the core – cladding mode coupling. The method for calculating the spectral characteristics of a grating described above ensures a good agreement between the calculated and experimental transmission spectra. At the exact resonance ($\delta = 0$) the energy exchange law is sinusoidal and it represents the feasibility of mutual transfer of energy from one mode to another:

$$R(z) = \cos^2(\eta z)\,, \qquad S(z) = \sin^2(\eta z)\,. \quad (7)$$

We can use the two expressions in Eqn (5) to find the total spectral width deduced from the first zero of the absorption spectrum:

$$\Delta\lambda = \frac{\lambda_r^2[\pi^2 - (\eta L)^2]^{1/2}}{\pi L(n_{\rm eff}^{\rm c} - n_{\rm eff}^{\rm cl})} = \frac{\lambda_r \Lambda[\pi^2 - (\eta L)^2]^{1/2}}{\pi L} \,. \qquad (8)$$

This relationship gives $\Delta\lambda \sim 15$ nm for a moderately strong mode interaction ($\eta L < \pi$) in a grating of length $L \sim 20$ mm formed in a fibre with the parameters given above. This value agrees well with $\Delta\lambda$ found experimentally.

3. Experiments

Long-period refractive-index gratings can be formed with an amplitude mask [6] or by successive imprinting of separate grating lines. The requirements which a UV radiation source must satisfy in order to be suitable for the formation of such gratings are less demanding than in the Bragg grating case; in particular, there are no fundamental limitations on the radiation coherence. In view of much longer periods, the requirements in respect of the mechanical stability of the grating-formation system are less stringent.

In our experiments we irradiated a germanosilicate fibre with KrF laser radiation ($\lambda = 248$ nm) through an amplitude mask with a period $\Lambda = 320$ μm. The UV radiation density on the fibre surface was increased by a cylindrical silica-glass lens with a focal length 100 mm, which made it possible to form a laser spot 20 mm long and 1 mm wide. The fibre being irradiated was placed parallel to the long axis of this spot. The energy density per pulse was $E_p \approx 300$ mJ cm^{-2} and the pulse repetition frequency was $f \approx 20$ Hz. The grating transmission spectrum was recorded directly during its formation with a spectrum analyser made by Anritsu Co. in which a tungsten halogen lamp was used as the probe radiation source.

As shown in Ref. [9], when gratings were formed through a mask, it was possible to control the UV-radiation-induced RI in the fibre core. The method proposed there was based on determination of the spectral shift $\Delta\lambda_r$ of the loss maximum at one of the resonances, associated unambiguously to the induced RI. This made it possible to check the validity of relationships (6) and (7) by experimental determination of the dependences $S(\Delta n)$ for the case of interaction between the HE_{11} and HE_{17} modes (Fig. 3). In accordance with the set of relationships (7), this dependence can be approximated satisfactorily by the function

$$S(\Delta n) = \sin^2(A\Delta n) \,, \qquad (9)$$

where $A = 4IL/\lambda_r \approx 2.5 \times 10^3$ [the expression for A is obtained from expression (6) bearing in mind that the profile of a grating line is rectangular and also that $d/(\Lambda - d) = 1$], which for $L = 20$ mm gives the overlap integral $I \approx 0.05$. The calculated value is $I = 0.053$.

As pointed out above, the usual diameter of a fibre cladding is sufficiently large and the cladding can guide a large number of modes, whereas the use of a long-period grating makes it possible to excite selectively a single cladding mode. This enabled us to determine experimentally the spatial distribution of the radiation intensity in the HE_{16} cladding mode.

We formed a grating in a fibre in which the interaction between HE_{11} and HE_{16} occurred at the laser diode wavelength 1.532 μm and the exchange of energy at this wavelength was $S \approx 10$ dB. The fibre was broken off directly behind the grating. Therefore, at the fibre end the radiation propagated mainly in the HE_{16} mode. The output radiation was analysed by the near-field method in an optical system with a magnification of $100^{\times}$ and a receiving aperture of 50 μm in diameter. Fig. 4 shows the spatial distribution of the intensity at the fibre exit determined in this way. As expected on the basis of our theoretical analysis, the distribution had a characteristic spatial size close to the fibre cladding diameter 125 μm, it had a strong axial symmetry, and exhibited radial oscillations whose number was less by unity than the radial order of the mode m (Fig. 1). The outer rings were not quite closed probably because of systematic experimental errors or because of relatively fast energy transfer to the cladding modes with similar propagation constants.

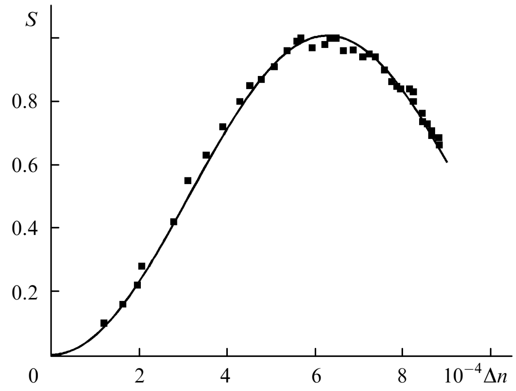

Figure 3. Dependence of the losses at the centre of the absorption band of a grating on the change in the refractive index.

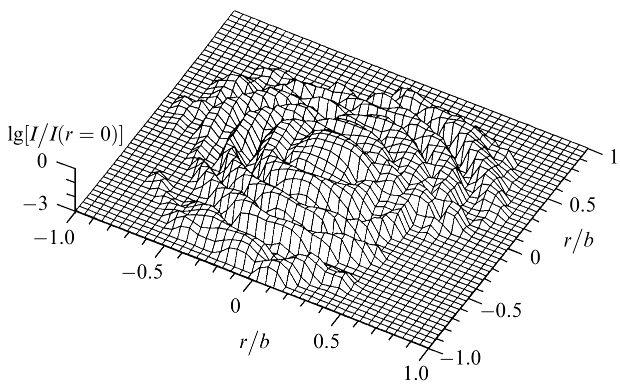

Figure 4. Experimentally determined spatial distribution of the intensity in the HE_{16} cladding mode.

4. Conclusions

We provided a mathematical description of the spectral characteristics of photoinduced in-fibre long-period RI gratings for coupling the core and cladding modes. We found that numerical calculations based on a simplified model of a three-layer fibre structure are in good agreement with the experimentally determined characteristics. The proposed description makes it possible to investigate theoretically the properties of long-period gratings and to predict their spectral characteristics.

References

1. Williams D L, Ainslie B J, Kashyap R, Maxwell G D, Armitage J R, Campbell R J, Wyatt R *Proc. SPIE Int. Soc. Opt. Eng.* **2044** 55 (1993)
2. Albert J, Malo B, Bilodeau F, Johnson D C, Hill K O, Hibino Y, Kawachi M *Opt. Lett.* **19** 387 (1994)
3. Kashyap R *Opt. Fiber Technol.* **1** (1) 17 (1994)
4. Vengsarkar A M, Lemaire P J, Judkins J B, Bhatia V, Erdogan T, Sipe J E *J. Lightwave Technol.* **14** 58 (1996)
5. Dianov E M, Karpov V I, Kurkov A S, Medvedkov O I, Prokhorov A M, Protopopov V N, Vasiliev S A *Meeting on the Photosensitivity and Quadratic Nonlinearity in Glass Waveguides: Fundamentals and Applications, Portland, OR, 1995* (OSA Technical Digest Series, Vol. 22) (Washington, DC: Optical Society of America, 1995) p. 14
6. Dianov E M, Kurkov A S, Medvedkov O I, Vasiliev S A, Paper presented at the Eurosensors X Conference, Leuven, Belgium, 1996, Paper P5.1
7. Unger H G *Planar Optical Waveguides and Fibres* (Oxford: Clarendon Press, 1978)
8. Tamir T (Ed.) *Integrated Optics* (Berlin: Springer, 1975)
9. Dianov E M, Kurkov A S, Medvedkov O I, Vasiliev S A *Meeting on the Photosensitivity and Quadratic Nonlinearity in Glass Waveguides: Fundamentals and Applications, Portland, OR, 1995* (OSA Technical Digest Series, Vol. 22) (Washington, DC: Optical Society of America, 1995) p. 104